

Ganymede: A new radio source

W. S. Kurth,¹ D. A. Gurnett,¹ A. Roux,² and S. J. Bolton³

Abstract. Observations by the Galileo plasma wave receiver during the first two flybys of Ganymede revealed that this Jovian moon is the source of narrowband electromagnetic radio waves, making it the only satellite in the solar system known to generate non-thermal radio emissions. The emissions are the result of mode-coupling from electrostatic electron cyclotron emissions near the upper hybrid resonance frequency, similar to non-thermal continuum radiation found at the known magnetized planets.

Introduction

Of the planets with known intrinsic magnetic fields (Mercury, Earth, Jupiter, Saturn, Uranus, and Neptune), all except Mercury are sources of nonthermal radio emissions [c.f. Kaiser, 1989]. Mercury is likely also a source, but no radio astronomy investigation has ever visited this planet and there are no Earth-based observations of Hermean radio emissions. Heretofore, no satellite of any of the planets has been found to be a source of radio emissions, although the strong influence of Io in the production of decametric radiation at Jupiter [Bigg, 1964] is well known. Now, however, with the discovery of a magnetosphere associated with Ganymede [Gurnett et al., 1996; Kivelson et al., 1996] clear evidence for radio emissions emanating directly from this magnetosphere has been found.

Radio emissions from planetary magnetospheres are currently classified in three categories by the generation mechanism thought to be responsible for the various emissions. The most intense emission at each of the planets is thought to be generated by the cyclotron maser instability [Wu and Lee, 1979] near the electron cyclotron frequency in the high magnetic latitude region. Auroral kilometric radiation at the Earth [Gurnett, 1974], Jovian decametric radiation, and Saturnian and Uranian kilometric radiation are all examples of this type of emission [Kaiser, 1989]. Neptune's higher frequency smooth and bursty emissions are also of this type [Zarka et al., 1995]. Generally speaking, there is either a demonstrable or suspected relationship between the cyclotron maser instability emissions and auroral processes in each of the planetary magnetospheres. The second type of emission is much less intense but just as ubiquitous. It has generally been termed nonthermal continuum radiation [Gurnett, 1975], myriametric radiation [Jones, 1988], or narrowband electromagnetic radiation [Gurnett et al., 1983] and is the result of the conversion of electrostatic waves at the upper hybrid resonance frequency into electromagnetic radio waves via either a linear [c.f.

Jones, 1988] and/or a nonlinear mechanism [c.f. Rönmark, 1992]. These emissions are typically generated at greater distances from the planet than the cyclotron maser emissions (e.g. at the plasmopause, plasmashet, or magnetopause) and, hence, are typically at lower frequencies. Especially at Earth and Jupiter a significant portion of the continuum spectrum is generated at frequencies below the surrounding solar wind plasma frequency and is therefore trapped within the magnetospheric cavity. Higher frequency components can escape the magnetosphere. The third known type of planetary radio emission is often called $2f_p$ emission from the planetary bow shock [Gurnett, 1975] and is the result of nonlinear interactions of Langmuir waves in the electron foreshocks of planetary magnetospheres which produce weak electromagnetic emissions at twice the electron plasma frequency in the foreshock [c.f. Cairns, 1988].

The radio emissions discussed here are of the second category. We will show using wave observations from the first two Galileo flybys of Ganymede that these emissions are clearly generated in the magnetosphere of Ganymede, that their source is associated with intense upper hybrid resonance bands in the magnetosphere, and that they are very similar to the terrestrial escaping nonthermal continuum (myriametric) radiation and the narrowband electromagnetic radiation at Jupiter and Saturn.

The Galileo plasma wave instrument utilizes an electric dipole antenna mounted on the end of the 10.6-m magnetometer boom with a length of approximately 6.6 m tip-to-tip. Search coil magnetometers covering the frequency range up to 160 kHz are also used, mounted on the high gain antenna feed. The plasma wave receiver consists of a 4-channel spectrum analyzer covering the range from 5.62 Hz to 31.1 Hz, a medium frequency receiver covering the range from 40 Hz to 160 kHz with 112 channels, and a high frequency receiver covering 100 kHz - 5.6 MHz with 42 channels. In essence, these 158 channels can be thought of as a single sweep frequency receiver which accumulates a complete spectrum every 18.67 seconds. For a more detailed description of the instrument, see Gurnett et al. [1992].

Observations

Figures 1 and 2 show frequency-time spectrograms summarizing the radio and plasma wave observations from the first and second Galileo flybys of Ganymede on June 27 and September 6, 1996. In these spectrograms we have plotted the intensity of the electric field component of the wave spectrum as a function of time (abscissa) and frequency (ordinate) using the color bar at the right to indicate intensity. Red areas represent the most intense wave features and blue the weakest. Spectrograms from the two flybys are remarkably similar and show the wealth of wave phenomena associated with the interaction between Ganymede's environment and the Jovian magnetosphere which led Gurnett et al. [1996] to conclude that the region was identical to a miniature planetary magnetosphere in numerous ways based solely on the plasma and radio waves observed.

¹Dept. of Physics & Astronomy, The University of Iowa

²Centre d'Etudes des Environnements Terrestre et Planétaires, Université Versailles

³Jet Propulsion Laboratory

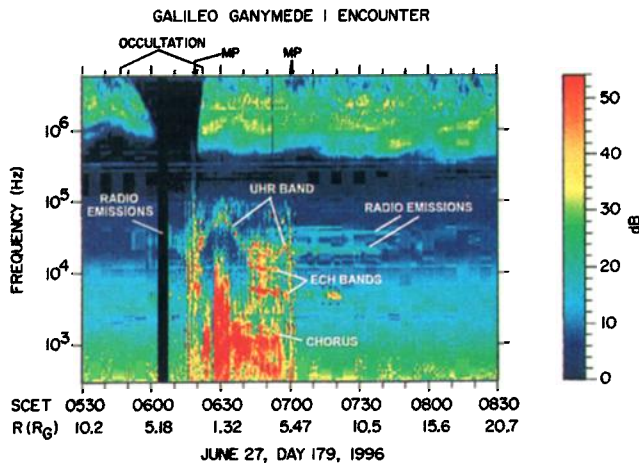


Figure 1. Frequency-time spectrogram summarizing the radio and plasma wave observations of the first Galileo flyby of Ganymede [after Gurnett et al. 1996]. Intensity of the electric field component of the wave spectrum is plotted as a function of time (abscissa) and frequency (ordinate) using the color bar at the right. Red areas represent the most intense wave features and blue the weakest. "MP" marks the locations of the inbound and outbound magnetopause crossings.

The two aspects of the wave spectra in Figures 1 and 2 which are most relevant to the Ganymede radio emissions are the radio emissions themselves and an intense band of electrostatic waves within the magnetosphere at the upper hybrid resonance frequency f_{UH} . The radio emissions are seen primarily on the outbound legs of the encounters, but weakly on the inbound leg of both encounters. For both encounters the emissions lie in the frequency range of approximately 15 to 50 kHz. There is also evidence for weak radio emissions up to about 100 kHz just above the upper hybrid resonance band during the first flyby. The upper hybrid band has been used by Gurnett et al. [1996] to obtain a density model for the plasma envelope near Ganymede. Since the upper hybrid frequency is simply a function of the electron plasma and cyclotron frequencies ($f_{UH}^2 = f_{pe}^2 + f_{ce}^2$), the frequency of the band can be used to determine f_{pe} . Since $f_{pe} = 8980\sqrt{n_e}$, where f_{pe} is in Hz and n_e is in cm^{-3} , the electron density is given directly if the magnetic field (hence f_{ce}) can be obtained from

the magnetometer. In the outer portion of Ganymede's magnetosphere, especially on the two outbound legs, is a region dominated by a series of banded emissions which lie between harmonics of the electron cyclotron frequency. These bands are often referred to as $(n+1/2)f_{ce}$ emissions or more simply electron cyclotron harmonic (ECH) emissions. The upper hybrid resonance band is a special case of the ECH emissions which occurs in the $(n+1/2)f_{ce}$ band including the upper hybrid resonance frequency [Kurth et al. 1979].

In the inner portion of Ganymede's magnetosphere, a single band is observed at high frequencies which Gurnett et al. [1996] identified as the upper hybrid band. The outbound outer portion of the magnetosphere shows emissions at the lower $(n+1/2)f_{ce}$ emissions as well. There is a brief interval of ECH wave activity just inside the inbound magnetopause in both encounter data sets.

High spectral resolution wideband data were obtained for both flybys with a bandwidth of 80 kHz. Fortunately, the wideband data from the second flyby extended to beyond both the inbound and outbound magnetopause crossings and reveal the radio emissions just outside Ganymede's magnetosphere. The electric field data are shown in Figure 3. The periodic gaps are time periods when the wideband receiver was connected to the magnetic antenna and configured with a 10-kHz bandwidth. The spectrogram is created through a series of Fourier transforms, hence, the frequency scale is linear instead of logarithmic as are those in Figures 1 and 2. The first ECH harmonic, commonly referred to as the $3f_{ce}/2$ band, is easily observed both inbound around 1851 spacecraft event time (SCET) and also outbound from about 1908 SCET to the magnetopause at 1923 SCET. The highest frequency band is denoted as the upper hybrid band. This band is quite bursty and extends well above the 80-kHz bandpass of the receiver near closest approach. At some times, such as near 1905 SCET the UHR band actually appears in two successive cyclotron harmonic bands. This can occur when the upper hybrid frequency lies very close to a cyclotron harmonic. Notice that two rather intense bands occur just prior to the outbound magnetopause crossing which are at nearly the same frequencies as the two radio emissions which appear just prior to the end of the spectrogram. Radio emissions which appear prior to the entry into the magnetosphere are more sporadic and variable in bandwidth. The bright (red), but very brief burst of UHR emission centered near 30 kHz at 1850 SCET may be related to these inbound radio emissions.

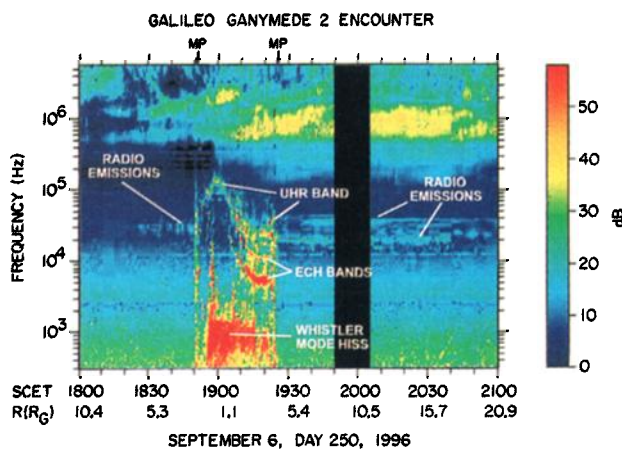


Figure 2. Spectrogram similar to Figure 1 but for the second Ganymede flyby.

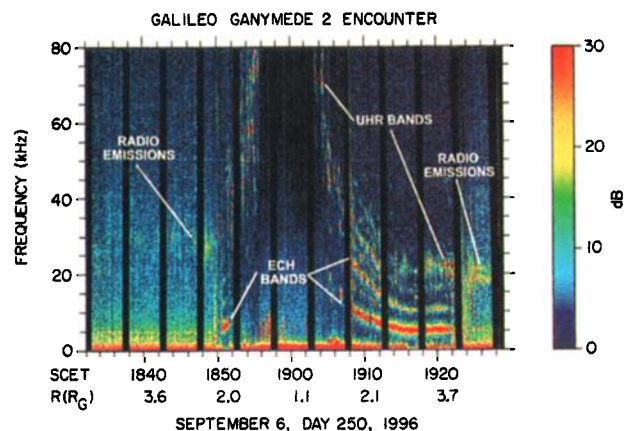


Figure 3. High spectral resolution wideband observations taken during the second flyby.

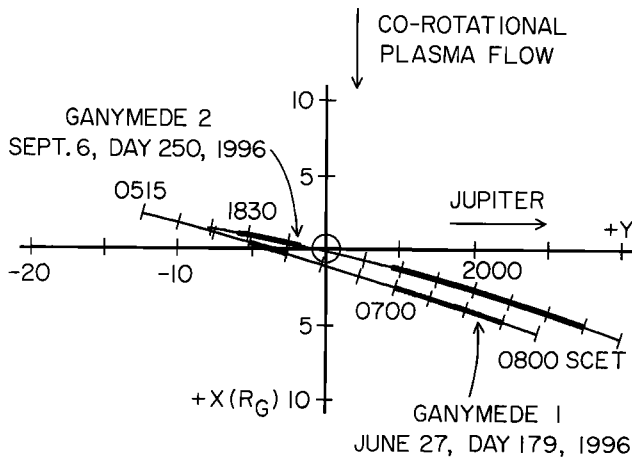


Figure 4. Schematic of the first two Ganymede flybys showing by the use of thick lines the regions in which Ganymede's radio emissions were observed.

The radio emissions extend to a distance of some 15–20 Ganymede radii R_G ($R_G = 2634$ km) in the direction of the outbound Galileo trajectory in both flybys (towards Jupiter) as shown in Figure 4. Here, we plot the trajectories of Galileo for the two flybys on a coordinate system centered at Ganymede and having x in the nominal plasma corotation direction and y in the direction towards Jupiter. The trajectory is represented by a thick line during times when the radio emissions are seen beyond the Ganymede magnetopause as identified by Gurnett et al. [1996]. The weak emissions above 50 kHz very close to Ganymede are not included here.

The emissions appear in two or three bands in the range of about 15 to 50 kHz. The bandwidths of each of the bands span from one to a few of the Galileo sweep frequency receiver's channels, or of the order of 10 percent of the frequency. In Figure 5 we show the power flux of radio emissions at 20.1 kHz as a function of radial distance taken from the first encounter's outbound observations. The alternating series of constant or sloping amplitudes is due to the amplitude inaccuracy introduced by the lossy Integer Cosine Transform used to compress these data in response to the failure of the Galileo high gain antenna. As can be seen in Figure 5, this results in errors of the order of ~ 5 dB. The rather sporadic, bursty behavior of the signals nearest Ganymede is likely due to electrostatic emissions in the magnetosphere of Ganymede. We attribute the local minimum in the signal at about $6.7 R_G$ to the spacecraft being both outside of the magnetosphere and temporarily shadowed from a radio emission beam. Just beyond $7 R_G$ however, the spacecraft is in a radio emission beam which decreases in intensity with distance (but subject to the data compression effects noted above). We initially assume that the source is between Ganymede and the spacecraft and fit to a curve for power flux P_f in $\text{W/m}^2\text{Hz}$ of the form $\log(P_f) = \log(P_o/(r-R_o)^2)$ to the data beyond about $7 R_G$ and obtained a reasonably good fit. P_o is the power emitted from the source in W/Hz , R_o is the source position and r is the position of Galileo as a function of time, both measured from Ganymede. The fit parameters $R_o = 5.43 \pm 0.30 R_G$ and $P_o = 8.32 \pm 1.4 \times 10^{-3} \text{ W/Hz}$ (assuming radiation into 2π steradians) are reasonably well-determined. This is an over-simplified construction, however, since the source is not directly between the spacecraft and Galileo, nor is the trajectory of the

spacecraft likely to be directly radial with respect to the source. We attempted to fit the same data with a function of the form $\log(P_f) = \log(P_o/((x-X_o)^2 + (y-Y_o)^2 + (z-Z_o)^2))$ where we use Cartesian coordinates with respect to Ganymede for the position of the source and Galileo. The curve derived for this fit is virtually identical to that shown in Figure 5, however, the parameters have extremely large (100 to 1000 times the parameter value) uncertainties due to strong dependencies between them. The position for the source obtained from this fit, ambiguous as it is, is at about $5.4 R_G$ from Ganymede and close to the Galileo trajectory. We take this as additional evidence that our assumption for nearly radial motion from the source for the fit in Figure 5 is not unwarranted and that the R_o derived from the simpler fit is consistent. This result is consistent with other arguments presented below that the 20-kHz source is likely near the magnetopause.

The determination of $P_o = 8.32 \times 10^{-3} \text{ W/Hz}$ gives a total power emitted of about 83 Watts (using an integrated bandwidth of about 10 kHz). Using the observed power flux of $6.2 \times 10^{-17} \text{ W/m}^2\text{Hz}$ at $7.2 R_G$, we find that the power flux at a standard distance of 1 astronomical unit (AU) is approximately $6 \times 10^{-26} \text{ W/m}^2\text{Hz}$. This can be compared to other planetary radio emissions and, according to Kaiser [1989], is $\sim 10^6$ less intense than the median power flux of Jovian narrowband kilometric radiation at 1 AU which is likely generated via a similar mechanism to these Ganymede emissions. Given the much smaller source size, one would expect such a minuscule value for Ganymede.

Generation Mechanism

The most obvious source of the Ganymede radio emissions are the upper hybrid resonance emissions in the Ganymede magnetosphere shown clearly in Figures 1–3. These are known to be the source of narrowband continuum radiation at Earth [Kurth et al. 1981] and narrowband electromagnetic bands at Jupiter [Gurnett et al., 1983]. Figure 6 shows a spectrum of the emissions observed at 0649:46 SCET just inside the outbound magnetopause during the first Ganymede flyby. The most intense peak here is near $300 \mu\text{V/m}$, similar to the intensity of the emissions at Earth. It is likely that even more intense bursts occur, perhaps into the mV/m range.

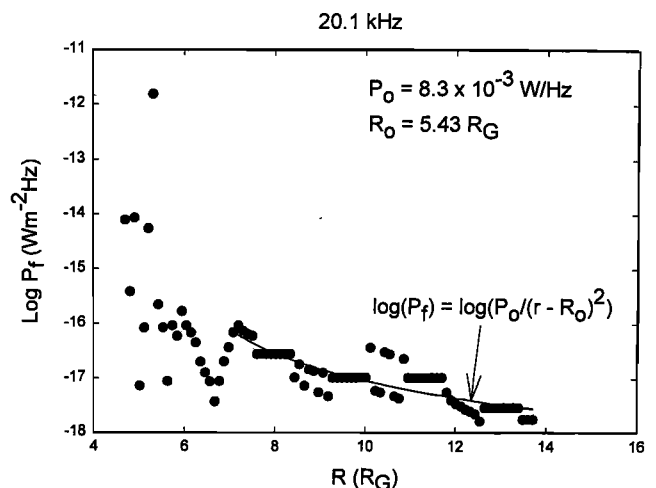


Figure 5. Power flux at 20.1 kHz versus distance from Ganymede showing that the radio emissions decrease in intensity as the inverse square of the distance from the source.

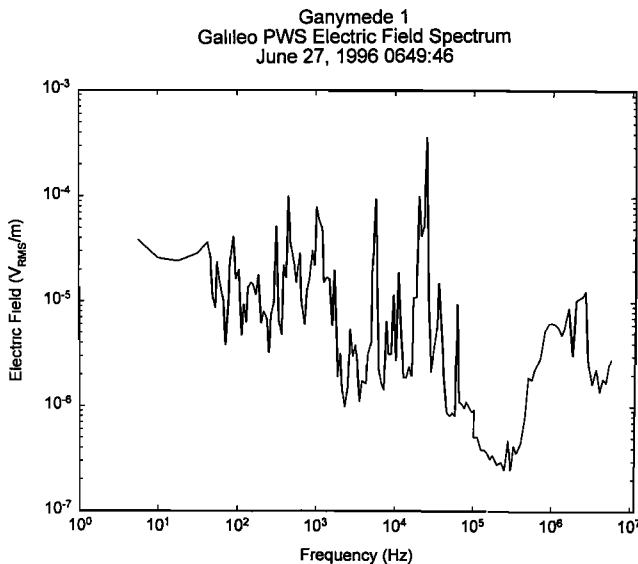


Figure 6. Electric field spectrum taken inside Ganymede's magnetosphere showing an electrostatic upper hybrid band with an intensity approaching 1 mV/m at about 25 kHz; this is a likely source for the narrowband Ganymede radio emissions.

(Recall that Galileo evidently did not pass directly through the source region.) The weak narrowband radio emissions observed at frequencies similar to those of electrostatic upper hybrid bands in Ganymede's magnetosphere leads to the straightforward conclusion that these emissions are similar to the escaping nonthermal continuum radiation at the Earth and narrowband electromagnetic emissions observed at Jupiter and the other outer planets. In these other examples, especially at Earth, it has been shown that the radio emissions are the result of mode conversion from the electrostatic mode to the electromagnetic mode [Jones, 1980; Kurth et al., 1981].

The fit of the spatial decrease in intensity to a source position near $5.4 R_G$ shown in Figure 5 places the source near the magnetopause. Also, the fact that the lower frequency emissions are in the same frequency range as the highest of the ECH bands in the outer Ganymede magnetosphere and typically not associated with the frequency of the peak of the upper hybrid band near closest approach implies the upper hybrid bands near the magnetopause are most likely to be involved in the generation of the lower frequency Ganymede radio emissions such as those near 20 kHz. The weak emissions above 50 kHz are found only near closest approach and are most likely generated at the upper hybrid frequency closer to Ganymede where the plasma density is greater.

Conclusions

The discovery of the Ganymede magnetosphere is among the most dramatic of the Galileo mission to date. That this magnetosphere is the source of nonthermal radio emissions is an example of the depth to which the magnetosphere of Ganymede encompasses the normal processes of planetary magnetospheres. Given the ubiquity of the continuum radiation at the known magnetized planets, it is not surprising to find such emissions. It is interesting, though, that the other, more intense magnetospheric emission is apparently not present. This is the cyclotron maser emission such as auroral kilometric radiation at Earth or the decametric and hectometric radiation at Jupiter. Given the large plasma

densities measured near Ganymede in the vicinity of its magnetic pole, the reason for the lack of the cyclotron maser instability is most likely due to the lack of an auroral cavity, or regime where $f_{pe}/f_{ce} \leq 0.3$ which is the criterion for X mode radiation at the Earth by this mechanism.

Acknowledgments. The research at The University of Iowa is supported by NASA through Contract 958779 through the Jet Propulsion Laboratory. The authors are grateful for the especially valuable comments from one of the referees.

References

- Bigg, E. K., Influence of the satellite Io on Jupiter's decametric emission, *Nature*, **203**, 1008-1010, 1964.
- Cairns, I. H., A semiquantitative theory for the $2f_p$ radiation observed upstream from the Earth's bow shock, *J. Geophys. Res.*, **93**, 3958-3968, 1988.
- Gurnett, D. A., The Earth as a radio source: Terrestrial kilometric radiation, *J. Geophys. Res.*, **79**, 4227-4238, 1974.
- Gurnett, D. A., The Earth as a radio source: The nonthermal continuum, *J. Geophys. Res.*, **80**, 2751-2763, 1975.
- Gurnett, D. A., W. S. Kurth, and F. L. Scarf, Narrowband electromagnetic emissions from Jupiter's magnetosphere *Nature*, **302**, 385-388, 1983.
- Gurnett, D. A., W. S. Kurth, R. R. Shaw, A. Roux, R. Gendrin, C. F. Kennel, F. L. Scarf, and S. D. Shawhan, The Galileo plasma wave investigation, *Space Sci. Rev.*, **60**, 341-355, 1992.
- Gurnett, D. A., W. S. Kurth, A. Roux, S. J. Bolton, and C. F. Kennel, Ganymede's magnetosphere: Galileo plasma wave observations, *Nature*, **384**, 535-537, 1996.
- Jones, D., Latitudinal beaming of planetary radio emissions, *Nature*, **288**, 225-229, 1980.
- Jones, D., Planetary radio emissions from low magnetic latitudes: Observations and theories, in *Planetary Radio Emissions II*, edited by H. O. Rucker, S. J. Bauer, and B. M. Pedersen, Austrian Academy of Sciences Press, Vienna, p. 255-293, 1988.
- Kaiser, M. L., Observation of non-thermal radiation from planets, in *Plasma Waves and Instabilities at Comets and in Magnetospheres*, edited by B. T. Tsurutani and H. Oya, American Geophysical Union, Washington, p. 221-237, 1989.
- Kivelson, M. G., K. K. Khurana, C. T. Russell, R. J. Walker, J. Warnecke, F. V. Coroniti, C. Polanskey, D. J. Southwood, and G. Schubert, Discovery of Ganymede's magnetic field by the Galileo spacecraft, *Nature*, **384**, 537-541, 1996.
- Kurth, W. S., J. D. Craven, L. A. Frank, and D. A. Gurnett, Intense electrostatic waves near the upper hybrid resonance frequency, *J. Geophys. Res.*, **84**, 4145-4164, 1979.
- Kurth, W. S., D. A. Gurnett, and R. R. Anderson, Escaping nonthermal continuum radiation, *J. Geophys. Res.*, **86**, 5519-5531, 1981.
- Rönnmark, K., Conversion of upper hybrid waves into magnetospheric radiation, in *Planetary Radio Emissions III*, edited by H. O. Rucker, S. J. Bauer, and M. L. Kaiser, Austrian Academy of Sciences Press, Vienna, p. 405-417, 1992.
- Wu, C. S., and L. C. Lee, A theory of the terrestrial kilometric radiation, *Astrophys. J.*, **230**, 621-626, 1979.
- Zarka, P., B. M. Pedersen, A. Lechacheux, M. L. Kaiser, M. D. Desch, W. M. Farrell, and W. S. Kurth, Radio emissions from Neptune, in *Neptune and Triton*, edited by D. P. Cruikshank, U. of Arizona, Tucson, p. 341-387, 1995.

W. S. Kurth and D. A. Gurnett, Dept. of Physics & Astronomy, The University of Iowa, Iowa City, IA 52242. (e-mail: william-kurth@uiowa.edu)

A. Roux, Centre d'Etudes des Environnements Terrestre et Planétaires, Université Versailles, Velizy, France. (e-mail: alain.roux@cetp.ipsl.fr)

S. J. Bolton, M.S. 169-506, Jet Propulsion Laboratory, Pasadena, CA, 91109. (e-mail: sbolton@gllsvc.jpl.nasa.gov)

(Received: February 28, 1997; revised: July 30, 1997; accepted: August 5, 1997.)